Theory of smectic A: A molecular model containing steric effects*

Legesse Senbetu and Chia-Wei Woo
Department of Physics and Astronomy, Northwestern University, Evanston, Illinois 60201
(Received 31 May 1977)

Starting with a pairwise, spatially and orientationally dependent intermolecular potential constructed to include steric effects, we carry out a systematic solution of the mean-field equation for liquid crystals. A model parameter which is connected to the molecular structure measures the strength of the steric forces. Its inclusion makes possible a semiquantitative comparison of our results to the experimentally obtained phase diagrams of several homologous series. The model predicts phase diagrams similar to that found by Lee *et al*. Improvements over the latter include (1) the characteristic feature of the smectic A phase, that the director prefers to be perpendicular to the smectic layers, arises naturally from our model; (2) the connection of one of our model parameters with the structure of molecules can now be used to explain the differences in phase-transition properties between homologous series whose molecules are of similar structure but differ in the length of the rigid section.

I. INTRODUCTION

Contributions to the molecular theory of smectic-A liquid crystals have been made by a number of investigators.[1-3] In all cases the treatments are extensions of the familiar Maier-Saupe[4] mean-field theory for nematics. The model interaction between a pair of molecules at positions $\vec{r}_1$ and $\vec{r}_2$, with respective orientations $\vec{\Omega}_1$ and $\vec{\Omega}_2$, is taken to be of the form

$$V(1,2) = V_0(r_{12}) + V_2(r_{12}) P_2(\hat{\Omega}_1 \cdot \hat{\Omega}_2). \tag{1.1}$$

The interaction potential defined in this manner depends on the magnitude of the vector $\vec{r}_{12}$ joining the molecular centers of mass, but not the orientation of $\vec{r}_{12}$ relative to the two molecular axes. As a result, for a fixed value of the relative orientation between $\hat{\Omega}_1$ and $\hat{\Omega}_2$, the model interaction given by Eq. (1.1) is spherically symmetric. This property results in a peculiar feature for the smectic phase, that the relative orientation between the director (the preferred direction of orientation of the molecular axis) and the direction of the density wave vector $\hat{q}$ (the normal to the smectic planes), is not uniquely determined. This means that it is equally favorable energetically for the director to lie in any direction. Such a model cannot distinguish smectic A from smectic C, nor can it exclude such unknown configurations in which the molecules lie laterally in smectic planes.

Recently a molecular statistical model for the smectic-A state based on a rank-two symmetry has been discussed.[5] The intermolecular potential assumed does not depend on the magnitude of the vector $\vec{r}_{12}$, but rather on its orientation relative to the two molecular axes. The peculiarity caused by the model given by Eq. (1.1) is then removed. But this model predicts a phase diagram which does not agree with experiment. The isotropic-smectic phase-transition boundary obtained is not an extension of the isotropic-nematic phase boundary.

The purpose of the present work is to propose a model constructed to take steric effects into account, and to study its implications via the mean-field theory. To include the short-range steric forces in our model, we follow the discussion given by Pople.[6] The pairwise interaction contains the desired properties mentioned above in that it depends on both the magnitude of $\vec{r}_{12}$ and the orientation of $\vec{r}_{12}$ relative to the axes of the two molecules. Thus, since it now contains all the relevant coordinates, the pairwise molecular interaction approximates the most general form for cylindrically symmetric molecules. It turns out that the model predicts phase diagrams in good qualitative and quantitative agreement with experiment. It also identifies the force which keeps the director oriented normal to the smectic layer: the mechanism that determines the energetically favored state as smectic A. We are able to connect the parameter which measures the strength of the steric effect to the length of the rigid section of the molecule. This relationship is further verified empirically by comparing our results with data for several homologous series.

The systematic and accurate procedure for solving mean-field equations as developed by Shen *et al*.[7] is used in this work.

II. PAIRWISE POTENTIAL

We assume that liquid crystals are composed of axially symmetric elongated organic molecules which do not have permanent dipole moments of consequence. In general six independent coordinates are required to specify the configuration of each rigid polyatomic molecule. These may be

taken as the Cartesian coordinates of some central point fixed in the molecule and three Eulerian angles: two to specify the direction of some fixed axis in the molecule, and the third to specify rotation about this body axis. The intermolecular energy will in general depend on all these coordinates. But for axially symmetric molecules the third Eulerian angle can be ignored.

Actually the most general form for the interaction potential between a pair of such molecules at positions $\vec{r}_1$ and $\vec{r}_2$, with orientations $\hat{\Omega}_1$ and $\hat{\Omega}_2$, is a function of five variables.[8] This follows from considerations of translational and rotational symmetries, which lead to the formation of the five scalars: r_{12}, $\hat{\Omega}_1 \cdot \hat{r}_{12}$, $\hat{\Omega}_2 \cdot \hat{r}_{12}$, $\hat{\Omega}_1 \cdot \hat{\Omega}_2$, and $\hat{\Omega}_1 \times \hat{\Omega}_2 \cdot \hat{r}_{12}$, with $\hat{\Omega}_i = (\theta_i, \varphi_i)$ as measured from some symmetry-breaking polar and azimuthal axis. The polar axis is usually called the "director" and denoted by the unit vector $\hat{n}$. The pseudoscalar $\hat{\Omega}_1 \times \hat{\Omega}_2 \cdot \hat{r}_{12}$ offers a selection between two signs. It gives rise to a chiral term. Assuming that the molecules are nonchiral, we need not consider the latter.[9]

Model systems with pairwise potential that depends only on the variables r_{12} and $\hat{\Omega}_1 \cdot \hat{\Omega}_2$ have been studied by many authors.[1-3] The potential is often written in the form

$$V(1,2) = V_0(r_{12}) + V_2(r_{12}) P_2(\hat{\Omega}_1 \cdot \hat{\Omega}_2). \tag{2.1}$$

We observe that such a potential gives the same value for the intermolecular potential between a pair of molecules with $\hat{\Omega}_1 \cdot \hat{r}_{12} = \hat{\Omega}_2 \cdot \hat{r}_{12} = 0$ and a pair with $\hat{\Omega}_1 \cdot \hat{r}_{12} = \hat{\Omega}_2 \cdot \hat{r}_{12} = 1$. But intuitively we expect that steric effects at play should lead to very different values for the two configurations. As a simple and straightforward generalization of Eq. (2.1), we shall now write our model potential as

$$V(1,2) = V_0(r_{12}) + V_2(r_{12}) P_2(\hat{\Omega}_1 \cdot \hat{\Omega}_2) + W_2(r_{12})[P_2(\hat{\Omega}_1 \cdot \hat{r}_{12}) + P_2(\hat{\Omega}_2 \cdot \hat{r}_{12})]. \tag{2.2}$$

The last two terms in Eq. (2.2) represent the simplest form of anisotropic intermolecular field that would account for steric forces between axially symmetric molecules.[6] The choice of the sign of $W_2(r_{12})$ will have consequences on phase transition properties. In making a choice we are guided by the following observation.

In order to have a stable smectic phase, we must clearly make the cohesive forces between molecules alongside each other strong enough to prevent them from moving out of the layers. This implies the existence of stronger cohesion operating between the sides of the molecules than between the ends of the molecules. Thus, based on properties of the terms between square brackets in Eq. (2.2), we require that on the average

$$W_2(r_{12}) > 0. \tag{2.3}$$

Now, if we choose the sign of $W_2(r_{12})$ according to Eq. (2.3), an increase in the value of W_2 increases the primary lateral attraction between molecules situated in a layer of the smectic. Thus with increasing W_2, the system becomes increasingly unstable against freezing within layers. A very strong W_2 leads to a smectic-B or a solid phase.

We assume $V_0(r)$ to be of the popular Lennard-Jones form,

$$V_0(r) = \eta[(\sigma/r)^{12} - (\sigma/r)^6], \tag{2.4}$$

and $V_2(r)$ and $W_2(r)$ to be Gaussian,

$$V_2(r) = -\delta\eta e^{-r^2/r_0^2}, \quad \delta > 0, \tag{2.5}$$

$$W_2(r) = \epsilon\eta e^{-r^2/r_0^2}, \quad \epsilon > 0. \tag{2.6}$$

We can gain some qualitative feelings about the potential by sketching profiles of $V(1,2)$. $V(1,2)$ depends on essentially four independent variables: (i) the angle between $\hat{\Omega}_1$ and $\hat{\Omega}_2$, (ii) the center-to-center distance r_{12} between the pair of molecules,

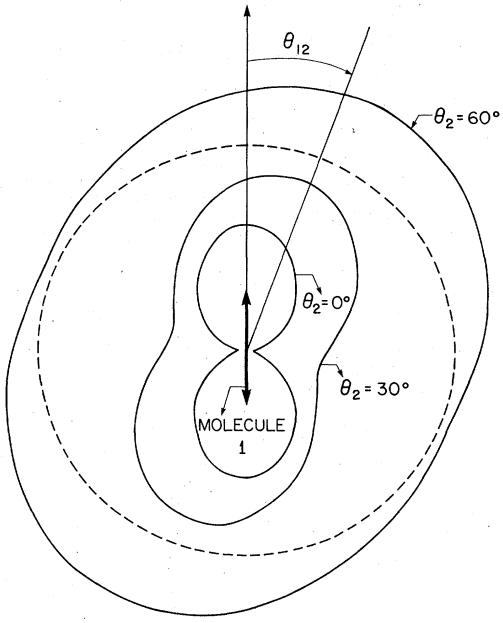

FIG. 1. Profile of the potential $V(1,2)$. The center-to-center distance between the two molecules is $r_{12} = 5$ Å. Molecule 1, with fixed orientation $\hat{\Omega}_1$, is located at the origin. θ_2 is the angle between $\hat{\Omega}_2$ and $\hat{\Omega}_1$. Each contour represents a plot of $V(1,2)$ vs the polar angle θ_{12} (the angle between $\hat{\Omega}_1$ and $\hat{r}_{12}$) for fixed θ_2. A point on each contour represents a value of $V(1,2)$ given (not to scale) by $V(1,2) = (r - R)$, where r and R represent radial distances from the origin to the contour point and the dashed circle, respectively.

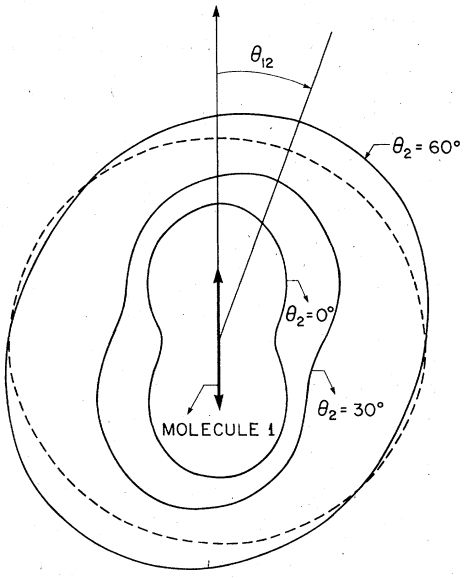

FIG. 2. Profile of the potential $V(1,2)$ for $r_{12}=15$Å. Molecule 1, whose orientation $\hat{\Omega}_1$ is fixed, is located at the origin. θ_2 is the angle between $\hat{\Omega}_2$ and Ω_1. Each contour represents a plot of $V(1,2)$ vs the polar angle θ_{12} (the angle between $\hat{\Omega}_1$ and $\hat{r}_{12}$) for fixed θ_2. A point on each contour represents a value of $V(1,2)$ given (not to scale) by $V(1,2)=r-R$ where r and R represent radial distances from the origin to the contour point and the dashed circle, respectively.

(iii) the angle between $\hat{\Omega}_1$ and $\hat{r}_{12}$, and (iv) the angle between $\hat{\Omega}_2$ and $\hat{r}_{12}$. A single plot of the profile of $V(1,2)$ showing the dependence on all the above variables is not easy. Thus, fixing the position and $\hat{\Omega}_1$ of the first molecule, we have made several qualitative plots of the angular and spatial dependence of $V(1,2)$ as shown in Figs. 1 and 2. Note that the profiles strongly suggest the inclusion of steric effects in our model.

Generally speaking, the form of $V_0(r)$ given by Eq. (2.4) is not amenable to easy mathematical manipulations. So for simplicity we will later assume a model potential with V_0 also given by a Gaussian. The spatial part of the model interaction between a pair of liquid-crystal molecules will then be of the form suggested originally by McMillan.[2] The anisotropic profile shown in Figs. 1 and 2 remains unchanged when this assumption is made.

In this paper we intend to examine the role played by the symmetry-breaking potential $W_2(r_{12})[P_2(\hat{\Omega}_1\cdot\hat{r}_{12})+P_2(\hat{\Omega}_2\cdot\hat{r}_{12})]$. In this manner we wish to learn to improve the model and strengthen the molecular basis of the theory of liquid crystals.

III. MEAN-FIELD EQUATIONS

For the sake of completeness we will summarize here the derivation and reduction of the mean-field equation.[7] Statistical mechanics begins with the partition function

$$Z=\int \exp\left(\frac{-1}{kT}\sum_{i<j}V(i,j)\right)\, d\vec{r}_1\, d\hat{\Omega}_1\ldots d\vec{r}_N\, d\hat{\Omega}_N. \quad (3.1)$$

We define the ν-particle distribution by

$$P^{(\nu)}(1,\ldots,\nu)=\frac{(4\pi)^\nu N!}{(N-\nu)!\,Z}\int \exp\left(\frac{-1}{kT}\sum_{i<j}V(i,j)\right) \times d\vec{r}_{\nu+1}\, d\hat{\Omega}_{\nu+1}\ldots d\vec{r}_N\, d\hat{\Omega}_N. \quad (3.2)$$

In particular we have the density function

$$P^{(1)}(1)\equiv P^{(1)}(\vec{r}_1,\hat{\Omega}_1)\equiv nf(\vec{r}_1,\hat{\Omega}_1) \equiv\frac{4\pi N}{Z}\int \exp\left(\frac{-1}{kT}\sum_{i<j}V(i,j)\right) \times d\vec{r}_2\, d\hat{\Omega}_2\ldots d\vec{r}_N\, d\hat{\Omega}_N, \quad (3.3)$$

and the pair distribution function

$$P^{(2)}(1,2)\equiv P^{(2)}(\vec{r}_1,\hat{\Omega}_1;\vec{r}_2,\hat{\Omega}_2) \equiv n^2 f(\vec{r}_1,\hat{\Omega}_1)f(\vec{r}_2,\hat{\Omega}_2)g(1,2) \equiv\frac{(4\pi)^2N(N-1)}{Z}\int \exp\left(\frac{-1}{kT}\sum_{i<j}V(i,j)\right) \times d\vec{r}_3\, d\hat{\Omega}_3\ldots d\vec{r}_N\, d\hat{\Omega}_N, \quad (3.4)$$

where $n=N/\mathcal{V}$ is the particle number density of the system and $g(1,2)$ is the pair correlation function.

Differentiating Eq. (3.3) with respect to spatial coordinates or angular coordinates gives rise to the integrodifferential equations:

$$\nabla_1 \ln f(r_1,\hat{\Omega}_1)=\frac{-n}{4\pi kT}\int f(\vec{r}_2,\hat{\Omega}_2)g(1,2) \times\nabla_1 V(1,2)\, d\vec{r}_2\, d\hat{\Omega}_2, \quad (3.5)$$

$$\nabla_{\Omega_1} \ln f(\vec{r}_1,\hat{\Omega}_1)=\frac{-n}{4\pi kT}\int f(\vec{r}_2,\hat{\Omega}_2)g(1,2) \times\nabla_{\Omega_1} V(1,2)\, d\vec{r}_2\, d\hat{\Omega}_2. \quad (3.6)$$

The solution of Eqs. (3.5) and (3.6) requires the knowledge of $g(1,2)$, which greatly complicates matters. But in the mean-field approximation, which does not take short-range correlations into account, so that $g(1,2)=1$, Eqs. (3.5) and (3.6) can be integrated directly to give

$$\ln[\lambda f(\vec{r}_1,\hat{\Omega}_1)]=\frac{-n}{4\pi kT}\int f(\vec{r}_2,\hat{\Omega}_2)V(1,2)\, d\vec{r}_2\, d\hat{\Omega}_2, \quad (3.7)$$

where $\ln\lambda$ is an integration constant.

Equation (3.7) is the mean-field equation, to be

reduced to a form that can be solved systematically. At this point we would like to point out that from the fact

$$\int P^{(1)}(\vec{r}_1, \hat{\Omega}_1)\, d\vec{r}_1\, d\hat{\Omega}_1 = 4\pi N, \tag{3.8}$$

we have the normalization condition,

$$\int f(\vec{r}, \hat{\Omega})\, d\vec{r}\, d\hat{\Omega} = 4\pi \mathcal{V}. \tag{3.9}$$

Let us assume a uniaxial distribution of molecules about the "director" $\hat{n}$. Also, we let the centers of molecules be located in planes normal to the Z axis of a fixed Cartesian coordinate system. Note that there has been no attempt to set $\hat{n}$ parallel to $\hat{Z}$. It is then natural to expand $f(\vec{r}, \hat{\Omega})$ in the form

$$f(\vec{r}, \hat{\Omega}) = f(z, \theta) = \sum_{p=-\infty}^{\infty} \sum_{l=1}^{\infty} \alpha_{p,2l} P_{2l}(\hat{n} \cdot \hat{\Omega}) e^{ipqZ}, \tag{3.10}$$

where q is related to the spacing d between planes ($d \geq 0$) by

$$q = 2\pi/d.$$

The coefficients $\alpha_{p,2l}$ are order parameters given by

$$\alpha_{p,2l} = \frac{4l+1}{4\pi \mathcal{V}} \int f(Z, \theta) P_{2l}(\hat{n} \cdot \hat{\Omega}) e^{-ipqZ} d\vec{r} \cdot d\hat{\Omega}. \tag{3.11}$$

Following Shen *et al.*[7] we introduce another set of parameters $\beta_{p,2l}$ by the definition

$$\ln[\lambda f(Z, \theta)] = \sum_{p=-\infty}^{\infty} \sum_{l=1}^{\infty} \beta_{p,2l} P_{2l}(\hat{n} \cdot \hat{\Omega}) e^{ipqZ}. \tag{3.12}$$

Utilizing the normalization condition (3.9), we obtain

$$\lambda = \frac{1}{4\pi \mathcal{V}} \int \exp\left(\sum_{p} \sum_{l=1}^{\infty} \beta_{p,2l} P_{2l}(\hat{n} \cdot \hat{\Omega}) e^{ipqZ} \right) d\vec{r} \cdot d\hat{\Omega}. \tag{3.13}$$

Now, making use of expression (2.2) for $V(1,2)$ and Eq. (3.10) on the right-hand side of Eq. (3.5), we find with the aid of the addition theorem of spherical harmonics:

$$\begin{aligned} \frac{\partial}{\partial Z_1} \ln f(Z_1, \theta_1) = {} & \frac{-n}{kT} \sum_{p=-\infty}^{\infty} \alpha_{p,0} \int e^{ipqZ_2} \frac{\partial}{\partial Z_1} V_0(r_{12})\, d\vec{r}_2 - \frac{n}{5kT} \sum_{p=-\infty}^{\infty} \alpha_{p,2} \int e^{ipqZ_2} P_2(\hat{n} \cdot \hat{\Omega}_1) \frac{\partial}{\partial Z_1} V_2(\vec{r}_{12})\, d\vec{r}_2 \\ & - \frac{n}{kT} \sum_{p=-\infty}^{\infty} \alpha_{p,0} \int e^{ipqZ_2} \frac{\partial}{\partial Z_1} [W_2(r_{12}) P_2(\hat{\Omega}_1 \cdot \hat{r}_{12})]\, d\vec{r}_2 \\ & - \frac{n}{5kT} \sum_{p} \alpha_{p,2} \int e^{ipqZ_2} \frac{\partial}{\partial Z_1} [W_2(r_{12}) P_2(\hat{n} \cdot \hat{r}_{12})]\, d\vec{r}_2. \end{aligned} \tag{3.14}$$

We next use Eq. (3.12) for $\ln f(Z, \theta)$ on the left-hand side of Eq. (3.14) and obtain after some straightforward algebra:

$$\beta_{p,0} = \frac{in}{kTpq} \left(\alpha_{p,0} \int e^{-ipqZ_{12}} \frac{\partial}{\partial Z_1} V_0(r_{12})\, d\vec{r}_2 + \frac{\alpha_{p,2}}{5} \int e^{-ipqZ_{12}} \frac{\partial}{\partial Z_1} \{W_2(r_{12}) P_2(\hat{n} \cdot \hat{r}_{12})\}\, d\vec{r}_2 \right), \tag{3.15}$$

$$\beta_{p,2} = \frac{in}{kTpq} \left(\frac{\alpha_{p,2}}{5} \int e^{-ipqZ_{12}} \frac{\partial}{\partial Z_1} V_2(r_{12})\, d\vec{r}_2 + \alpha_{p,0} \int e^{-ipqZ_{12}} \frac{\partial}{\partial Z_1} \{W_2(r_{12}) P_2(\hat{n} \cdot \hat{r}_{12})\}\, d\vec{r}_2 \right), \tag{3.16}$$

and $\beta_{p,l} = 0, l > 2$. The coefficients of order $l > 2$ vanish because of the truncated form of the potential given in Eq. (2.2).

To proceed further we must make an assumption about the explicit form of the short-range central forces. We take simply the Gaussian

$$\begin{aligned} V_0(r) &= -v_0 \delta e^{-r^2/r_0^2}, \\ V_2(r) &= -v_0 e^{-r^2/r_0^2}, \\ W_2(r) &= v_0 \epsilon e^{-r^2/r_0^2}, \end{aligned} \tag{3.17}$$

where r_0 gives the range of the potential and δ and ϵ measure the strength of V_0 and W_2 relative to V_2. $\epsilon > 0$ since $W_2 > 0$.

On the right-hand side of Eqs. (3.15) and (3.16), we now have integrals of the form

$$i \int e^{-ipqZ_{12}} \frac{\partial}{\partial Z_1} V_0(r_{12})\, d\vec{r}_2 = pq v_0 \delta \pi^{3/2} r_0^3 e^{-p^2 q^2 r_0^2/4} \tag{3.18}$$

and

$$i\int e^{-ipqZ_{12}}\frac{\partial}{\partial Z_1}[W_2(r_{12})P_2(\hat{n}\cdot\hat{r}_{12})]d\vec{r}_2$$
$$=4\pi pqv_0\epsilon\int_0^\infty e^{-(r/r_0)^2}j_2(pqr)P_2(\hat{n}\cdot\hat{Z})r^2\,dr$$
$$=(pq)^3v_0\epsilon\pi^{3/2}r_0^5[P_2(\hat{n}\cdot\hat{Z})/10]M(\tfrac{5}{2};\tfrac{7}{2};-p^2q^2r_0^2/4), \tag{3.19}$$

where $j_2(r)$ is the spherical Bessel function of order 2 and M is the confluent hypergeometric function. In evaluating the integral in Eq. (3.19), we used the expansion[10]:

$$e^{-ipqZ_{12}}=4\pi\sum_{l=0}^{\infty}\sum_{m=-l}^{l}(-i)^l j_l(pqr_{12})\times Y_l^m(\theta_q,\varphi_q)Y_l^{m*}(\theta_{12},\varphi_{12}). \tag{3.20}$$

Now using the Kummer transformation[11] we can write

$$M(\tfrac{5}{2},\tfrac{7}{2};-p^2q^2r_0^2/4)=e^{-p^2q^2r_0^2/4}M(1,\tfrac{7}{2};p^2q^2r_0^2/4). \tag{3.21}$$

Substituting the results (3.18), (3.19), and (3.21) in Eqs. (3.15) and (3.16) leads to

$$\beta_{p,0}=(v_0\pi^{3/2}r_0^3n/kT)\{\alpha_{p,0}\delta+\tfrac{1}{5}\alpha_{p,2}r_0^2\epsilon(pq)^2[P_2(\hat{n}\cdot\hat{Z})/10]M(1,\tfrac{7}{2};p^2q^2r_0^2/4)\}e^{-p^2q^2r_0^2/4}, \tag{3.22}$$
$$\beta_{p,2}=(v_0\pi^{3/2}r_0^3n/kT)\{\tfrac{1}{5}\alpha_{p,2}+\alpha_{p,0}r_0^2\epsilon(pq)^2[P_2(\hat{n}\cdot\hat{Z})/10]M(1,\tfrac{7}{2};p^2q^2r_0^2/4)\}e^{-p^2q^2r_0^2/4}, \tag{3.23}$$
$$\beta_{p,l}=0,\quad l>2. \tag{3.24}$$

From Eqs. (3.11)–(3.13) we also have

$$\alpha_{p,2l}=(4l+1)\frac{\int_{\Delta v}\int_{\Omega}\exp\left[\sum_{p'}\sum_{l'}\beta_{p',2l'}P_{2l'}(\hat{n}\cdot\hat{\Omega})e^{ip'qZ}\right]P_{2l}(\hat{n}\cdot\hat{\Omega})e^{-ipqZ}d\vec{r}\,d\hat{\Omega}}{\int_{\Delta v}\int_{\Omega}\exp\left[\sum_{p'}\sum_{l'}\beta_{p',2l'}P_{2l'}(\hat{n}\cdot\hat{\Omega})e^{ip'qZ}\right]d\hat{r}\,d\hat{\Omega}}, \tag{3.25}$$

with Δv denoting the volume of a unit cell. Thus instead of solving the mean-field equation directly our problem reduces to solving Eqs. (3.22)–(3.25) self-consistently. Let us next digress to discuss the physical properties of the model potential assumed in Eq. (3.17).

IV. FEATURES OF THE GAUSSIAN MODEL

Combining Eqs. (2.2) and (3.17) the short-ranged pairwise potential can be written as

$$V(1,2)=v_0\exp[-(r_{12}/r_0)^2]\times[-\delta-P_2(\hat{\Omega}_1\cdot\hat{\Omega}_2)+\epsilon P_2(\hat{\Omega}_1\cdot\hat{r}_{12})+\epsilon P_2(\hat{\Omega}_2\cdot\hat{r}_{12})]. \tag{4.1}$$

Thus four physical parameters enter the theory: v_0, δ, ϵ, and r_0. v_0 determines the nematic-isotropic transition temperature T_{IN}. r_0 is of the order of the length of the rigid section of the elongated organic molecule. It gives the range of the interaction. The effect of the parameters δ and ϵ is not very obvious. To gain some insight into the salient features of Eq. (4.1), let us make several observations about the experimental situation. The reader will find Fig. 3 helpful in following the discussion below.

Experimental phase diagrams of the transition temperatures with respect to number of carbons in the end alkyl chain, which we consider to be the chain length, show the following features. For short chain lengths, the smectic-A–nematic transition temperature T_{NA} increases with increasing chain length. T_{NA} rises and meets the nematic-isotropic transition temperature T_{IN}. For large chain lengths one has only the smectic-A and isotropic phases and the transition temperature T_{IA} generally decreases. Finally we observe that different classes of homologous series have in gen-

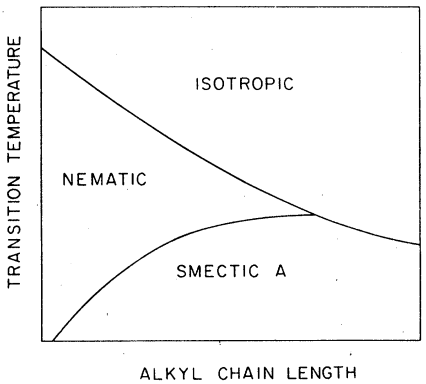

FIG. 3. Typical phase diagram for homologous series of compounds showing transition temperature vs length of alkyl end chains (Ref. 2).

eral a triple point at about the same end chain length.

With the above experimental results in mind let us now inspect the pairwise potential Eq. (4.1). The underlying idea for the discussion that follows has already been given.[3] First, let us consider the spatial part only for fixed δ and ϵ. The potential V_i seen by a single molecule i is approximately given by a summation of $V(i,j)$ over all molecules j sitting on planes spaced d apart. V_i is an oscillating function with periodic wells centered on the smectic planes and barriers arising from overlapping Gaussian tails. For chains which are sufficiently short, the height of the barriers increases with increasing chain length while the Gaussians disengage. This enhances the tendency of each molecule to be localized on a plane. Thus the transition temperature T_{NA} rises. As the chains continue to grow, eventually molecules are spaced too far apart for this mechanism to remain effective. Therefore T_{NA} and subsequently T_{IA} should stay constant with respect to chain length.

Also, according to Eq. (4.1) the strength of the orientational force diminishes as the average distance between molecules increases. Thus molecular alignment becomes more difficult as the chains lengthen. This results in a depression of the transition temperatures T_{IN} and T_{IA}, from isotropic to orientationally ordered states in a continuous manner.

In the region of intermediate chain length the magnitude of the parameters δ and ϵ gives rise to some features which could make the model inconsistent with experiment. So let us first consider a variation in the parameter δ. As δ increases, the wells centered at each plane become deeper. This enhances the tendency of each molecule to be localized on a plane. Thus, for short chains, the transition temperature T_{NA} rises with increasing δ. Now, for each δ there is a chain length L_δ at which T_{NA} meets T_{IN}. According to the above consideration, L_δ decreases. So for large δ, L_δ may not be large enough for the molecules to be considered far apart. As the chain length increases, T_{IA} will then *increase* until it becomes a constant finally. This is inconsistent with experimental observation. So contrary to the suggestion[3] that T_{IA} will decrease with increasing δ, we must limit the value of δ to small enough values if the model is to be consistent with experimental observations. The parameter δ thus helps determine T_{NA}, T_{IA}, and the triple point.

Finally we refer the reader to the discussion in the Sec. II for the origin of the parameter ϵ. It determines the transition temperature T_{NA}. But since most of the features of the experimental phase diagram are already reproduced by the previous model,[3] we expect ϵ to be much less than δ.

V. FURTHER REDUCTION OF MEAN-FIELD EQUATIONS

For simplicity we keep only the first Fourier coefficient and consider β_{00}, $\beta_{1,0}=\beta_{-1,0}$, $\beta_{0,2}$, and $\beta_{1,2}=\beta_{-1,2}$. Then from the self-consistency Eq. (3.25) we find

$$\alpha_{1,0}=\frac{\int_\Delta\int_\Omega \exp\{2\beta_{1,0}\cos(2\pi Z/d)+[\beta_{0,2}+2\beta_{1,2}\cos(2\pi Z/d)]P_2(\hat{n}\cdot\hat{\Omega})\}\cos(2\pi Z/d)\,d\vec{r}\,d\hat{\Omega}}{\int_{\Delta v}\int_\Omega \exp\{2\beta_{1,0}\cos(2\pi Z/d)+[\beta_{0,2}+2\beta_{1,2}\cos(2\pi Z/d)]P_2(\hat{n}\cdot\hat{\Omega})\}d\vec{r}\,d\hat{\Omega}}\,, \tag{5.1}$$

$$\alpha_{0,2}=5\,\frac{\int_{\Delta v}\int_\Omega \exp\{2\beta_{1,0}\cos(2\pi Z/d)+[\beta_{0,2}+2\beta_{1,2}\cos(2\pi Z/d)]P_2(\hat{n}\cdot\hat{\Omega})\}P_2(\hat{n}\cdot\hat{\Omega})\,d\vec{r}\,d\hat{\Omega}}{\int_{\Delta v}\int_\Omega \exp\{2\beta_{1,0}\cos(2\pi Z/d)+[\beta_{0,2}+2\beta_{1,2}\cos(2\pi Z/d)]P_2(\hat{n}\cdot\hat{\Omega})\}d\vec{r}\,d\hat{\Omega}}\,, \tag{5.2}$$

$$\alpha_{1,2}=5\,\frac{\int_{\Delta v}\int_\Omega \exp\{2\beta_{1,0}\cos(2\pi Z/d)+[\beta_{0,2}+2\beta_{1,2}\cos(2\pi Z/d)]P_2(\hat{n}\cdot\hat{\Omega})\}\cos(2\pi Z/d)P_2(\hat{n}\cdot\hat{\Omega})\,d\vec{r}\,d\hat{\Omega}}{\int_{\Delta v}\int_\Omega \exp\{2\beta_{1,0}\cos(2\pi Z/d)+[\beta_{0,2}+2\beta_{1,2}\cos(2\pi Z/d)]P_2(\hat{n}\cdot\hat{\Omega})\}d\vec{r}\,d\hat{\Omega}}\,. \tag{5.3}$$

Note that since the angular and the spatial parts are coupled, the above integrals cannot be evaluated in closed form. It is, however, possible to rewrite the various integrals in forms more amenable to numerical integration. In Appendix A it is shown that the integrals in Eqs. (5.1)–(5.3) can be expressed in terms of Dawson integrals. Then using the results (A1)–(A5) we obtain from Eqs. (5.1)–(5.3):

$$\alpha_{1,0}=\frac{\kappa_{10}(\beta_{0,2},\beta_{1,0},\beta_{1,2})}{\kappa_0(\beta_{0,2},\beta_{1,0},\beta_{1,2})}\,, \tag{5.4}$$

$$\alpha_{0,2}=5\,\frac{\kappa_{02}(\beta_{0,2},\beta_{1,0},\beta_{1,2})}{\kappa_0(\beta_{0,2},\beta_{1,0},\beta_{1,2})}\,, \tag{5.5}$$

$$\alpha_{1,2}=5\,\frac{\kappa_{12}(\beta_{0,2},\beta_{1,0},\beta_{1,2})}{\kappa_0(\beta_{0,2},\beta_{1,0},\beta_{1,2})}\,. \tag{5.6}$$

Now defining

$$t=kT/v_0, \quad n=n_x n_y n_z=\frac{1}{d_x}\frac{1}{d_y}\frac{1}{d},$$

and

$$\zeta_x=2\pi r_0/d_x, \quad \zeta_y=2\pi r_0/d_y, \quad \zeta=2\pi r_0/d, \tag{5.7}$$

and substituting them into Eqs. (3.22) and (3.23) we get

$$\beta_{1,0}=\frac{\zeta_x\zeta_y\zeta\delta}{8\pi^{3/2}t\kappa_0(\beta_{0,2},\beta_{1,0},\beta_{1,2})} \times\{\kappa_{10}(\beta_{0,2},\beta_{1,0},\beta_{1,2})+\frac{\epsilon\zeta^2}{\delta}\kappa_{12}(\beta_{0,2},\beta_{1,0},\beta_{1,2}) \times[P_2(\hat{n}\cdot\hat{Z})/10]M(1,\tfrac{7}{2};\zeta^2/4)\}e^{-\zeta^2/4}, \tag{5.8}$$

$$\beta_{1,2}=\frac{\zeta_x\zeta_y\zeta}{8\pi^{3/2}t\kappa_0(\beta_{0,2},\beta_{1,0},\beta_{1,2})} \times\{\kappa_{12}(\beta_{0,2},\beta_{1,0},\beta_{1,2})+\epsilon\zeta^2\kappa_{10}(\beta_{0,2},\beta_{1,0},\beta_{1,2}) \times[P_2(\hat{n}\cdot\hat{Z})/10]M(1,\tfrac{7}{2};\zeta^2/4)\}e^{-\zeta^2/4}, \tag{5.9}$$

$$\beta_{0,2}=\frac{\zeta_x\zeta_y\zeta}{8\pi^{3/2}t}\frac{\kappa_{02}(\beta_{0,2},\beta_{1,0},\beta_{1,2})}{\kappa_0(\beta_{0,2},\beta_{1,0},\beta_{1,2})}. \tag{5.10}$$

The expressions for κ_0, κ_{10}, κ_{12}, and κ_{02} can be evaluated easily by numerical integration using the Gauss-Chebyshev formula. So, for chosen t, ζ_x, ζ_y, and ζ, the coefficients β_{02}, β_{10}, and β_{12} can be evaluated by using a fixed-point iteration procedure from Eqs. (5.8)–(5.10).

It should be noted that β_{ij} depends explicitly on the value of the angle between the director and the direction of the density wave vector $\vec{q}$, denoted by $\hat{Z}$. This will help us to find out if our model allows for stable phases in which the director inclines at an angle relative to the Z axis. (For this purpose the Helmholtz free energy must be calculated and minimized.) In fact this feature renders our model as an improvement over previous models. In the models[1-3] studied previously it had usually been assumed that the direction of the density wave lies in the direction of the nematic preferred axis. But it is equally favorable energetically for $\hat{n}$ to be in any direction with respect to $\hat{Z}$. In the present model, this restriction has been removed in a very simple and natural way. It has been suggested[2] that if one considers excluded volume effect, the ambiguity concerning which direction of the director should give minimum free energy will be removed. Since in our model we have effectively accounted for steric effects, our results will offer a test of the above conjecture.

VI. FREE ENERGY

In the mean-field approximation the Helmholtz free-energy functional can be expressed as

$$\mathcal{F}=\mathcal{F}_0+\frac{kTn}{4\pi}\int f(\vec{r},\hat{\Omega})\ln\left(\frac{nf(\vec{r},\hat{\Omega})}{4\pi}\right)d\vec{r}\,d\hat{\Omega}+\frac{n^2}{32\pi^2}\int f(\vec{r}_1,\hat{\Omega}_1)f(\vec{r}_2,\hat{\Omega}_2)V(1,2)\,d\vec{r}_1 d\hat{\Omega}_1\,d\vec{r}_2\,d\hat{\Omega}_2. \tag{6.1}$$

From Sec. V, we have

$$f(z,\theta)=2\pi\frac{\exp\{2\beta_{1,0}\cos(2\pi Z/d)+[\beta_{0,2}+2\beta_{1,2}\cos(2\pi Z/d)]P_2(\hat{n}\cdot\hat{\Omega})\}}{e^{\beta_{0,2}}\kappa_0(\beta_{0,2},\beta_{1,0},\beta_{1,2})}. \tag{6.2}$$

Thus, using Eqs. (A1)–(A5), we obtain

$$\frac{kTn}{4\pi}\int f(\vec{r},\hat{\Omega})\ln\left(\frac{nf(\vec{r},\hat{\Omega})}{4\pi}\right)d\vec{r}\,d\hat{\Omega}=kTN\ln(\tfrac{1}{2}n)-kTN\ln\kappa_0(\beta_{0,2},\beta_{1,0},\beta_{1,2})-kTN\beta_{0,2} +\frac{kTN}{\kappa_0(\beta_{0,2},\beta_{1,0},\beta_{1,2})}[2\beta_{1,0}\kappa_{10}(\beta_{0,2},\beta_{1,0},\beta_{1,2})+\beta_{0,2}\kappa_{02}(\beta_{0,2},\beta_{1,0},\beta_{1,2}) +2\beta_{1,2}\kappa_{12}(\beta_{0,2},\beta_{1,0},\beta_{1,2})]. \tag{6.3}$$

The next step is to consider the third term in the free-energy functional expression (6.1):

$$F_2\equiv\frac{n^2}{32\pi^2}\int f(\vec{r}_1,\hat{\Omega}_1)f(\vec{r}_2,\hat{\Omega}_2)V(1,2)\,d\vec{r}_1 d\hat{\Omega}_1\,d\vec{r}_2\,d\hat{\Omega}_2. \tag{6.4}$$

F_2 is a complicated integral and cannot be evaluated in a closed form. In Appendix B we use Eq. (6.2) to write F_2 in a form that can easily be integrated numerically. The results from Eqs. (6.3) and (B12) can now be put into Eq. (6.1) to give the Helmholtz free-energy functional:

$$\mathfrak{F} = \mathfrak{F}_0 + kTN\Big(\ln(\tfrac{1}{2}n) - \beta_{02} - \ln\kappa_0(\beta_{02},\beta_{10},\beta_{12}) + \frac{1}{\kappa_0(\beta_{02},\beta_{10},\beta_{12})}[2\beta_{10}\kappa_{10}(\beta_{02},\beta_{10},\beta_{12}) + \beta_{02}\kappa_{02}(\beta_{02},\beta_{10},\beta_{12}) + 2\beta_{12}\kappa_{12}(\beta_{02},\beta_{10},\beta_{12})] + \frac{\zeta_x\zeta_y}{4\pi t[\kappa_0(\beta_{02},\beta_{10},\beta_{12})]^2}[-\tfrac{1}{2}\delta J_0(\beta_{02},\beta_{10},\beta_{12};\zeta) - \tfrac{1}{2}J_2(\beta_{02},\beta_{10},\beta_{12};\zeta) + (2\epsilon/\zeta^2)J_3(\beta_{02},\beta_{10},\beta_{12};\zeta)]\Big). \quad (6.5)$$

VII. NUMERICAL RESULTS AND COMPARISON WITH EXPERIMENT

In performing numerical work we choose the parameters ζ_x and ζ_y to be

$$\zeta_x = \zeta_y = \pi.$$

We also assume values for the potential strengths δ and ϵ. Then for each value of the parameter ζ^{-1}, which characterizes the chain length and takes the role of volume in a thermodynamic sense, each value of the reduced termperature t, and each value of $(\hat{n}\cdot\hat{Z})$, which should also be viewed as a thermodynamic variable, we use fixed-point iteration to evaluate the coefficients $\beta_{0,2}$, $\beta_{1,0}$, and $\beta_{1,2}$. For the isotropic phase, $\beta_{0,2}=\beta_{1,0}=\beta_{1,2}=0$. For the nematic phase, $\beta_{0,2}\neq 0$ and $\beta_{1,0}=\beta_{1,2}=0$. And for the smectic phase, $\beta_{0,2}\neq 0$, $\beta_{1,0}\neq 0$, and $\beta_{1,2}\neq 0$. The computed values of $\beta_{1,0}$, $\beta_{0,2}$, and $\beta_{1,2}$ are used to evaluate the Helmhotz free energy. For each chosen value of ζ^{-1}, the stable phase (isotropic, nematic, or smectic) is then determined by comparing the free energies in the three phases at the same temperature t. Furthermore, a comparison of the free energies for different values of $(\hat{n}\cdot\hat{Z})$ will give the angle between $\hat{n}$ and $\hat{Z}$ which minimizes the free energy. Our numerical results always gave $(\hat{n}\cdot\hat{Z})=1$, which means that only one direction of $\hat{n}$ with respect to $\hat{Z}$ is energetically favorable.

In this manner the transition temperatures T_{IN}, T_{NA}, and T_{IA} as functions of ζ^{-1} can be determined and the "phase diagram" drawn. The procedure is then repeated for different combinations of δ and ϵ.

As was pointed out earlier, the theory has four interaction parameters: v_0, δ, ϵ, and r_0, which we fix by requiring the model to fit the measured transition-temperature curves and approximate triple point. For each homologous series, our variation of v_0 determines one point on the transition-temperature curve $T_{IN}(\zeta^{-1})$, while r_0 measures the length of the central section of the molecule. Both these parameters are chosen at the outset and thereafter held fixed. Only the parameters δ and ϵ remain at our disposal to be varied in order to fit the rest of the experimental phase diagram.

There have been extensive measurements of liquid-crystal "phase diagrams" for different homologous series of compounds. Transition temperatures as functions of the number of carbon atoms in the alkyl end chain have been obtained. To fit the experimental data we locate a value of δ that gives simultaneously the best possible fit to the isotropic-nematic transition curve and the approximate triple point. Then, for that δ, we select a value of ϵ which gives T_{NA} closest to the experimental curve. In this manner we obtain semiphenomenological theoretical phase diagrams. These calculations were done and compared to experimental data on five homologous series: 4-ethoxybenzal-4-amino-*n*-alkyl-α-methylcinamates,[13] *p*-*n*-alkozybenzylidene-*p*-aminobenzoic acids,[14] 4-*p*-*n*-alkoxybenzylidene-aminodiphenyls,[15] 4-*n*-alkoxy-

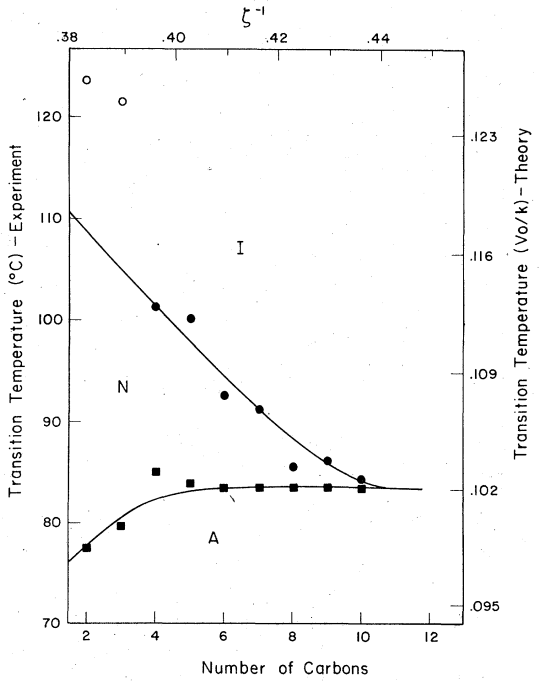

FIG. 4. Comparison of theoretical phase diagram with experiment for homologous series 4-ethoxybenzal-4-amino-*n*-alkyl-α-methylcinemates. Solid lines are from the theoretical model with $\delta=0.45$ and $\epsilon=0.03$. Filled circles denote experimental nematic-isotropic transition temperatures; squares denote nematic-smectic-*A* transition temperatures from Ref. 13.

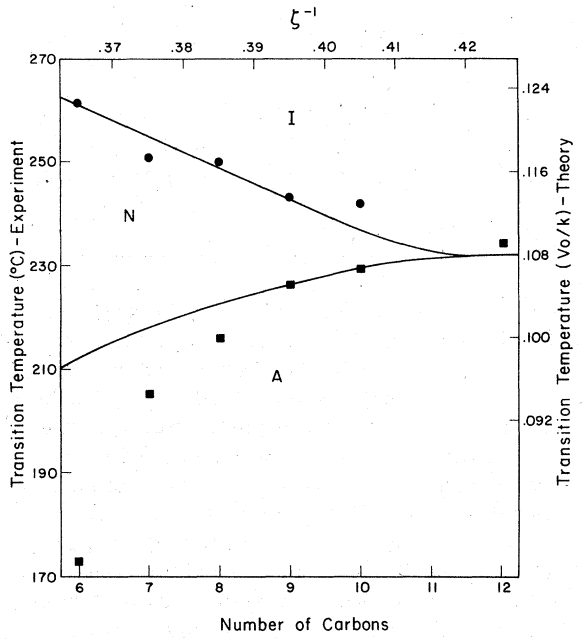

FIG. 5. Comparison of theoretical phase diagram with experiment for homologous series p-n-alkoxybenzylidene-p-aminobenzoic acids. Solid lines are from the present model with $\delta = 0.65$ and $\epsilon = 0.0$. Filled circles and squares denote experimental nematic-isotropic and nematic–smectic-A transition temperatures, respectively, from Ref. 15.

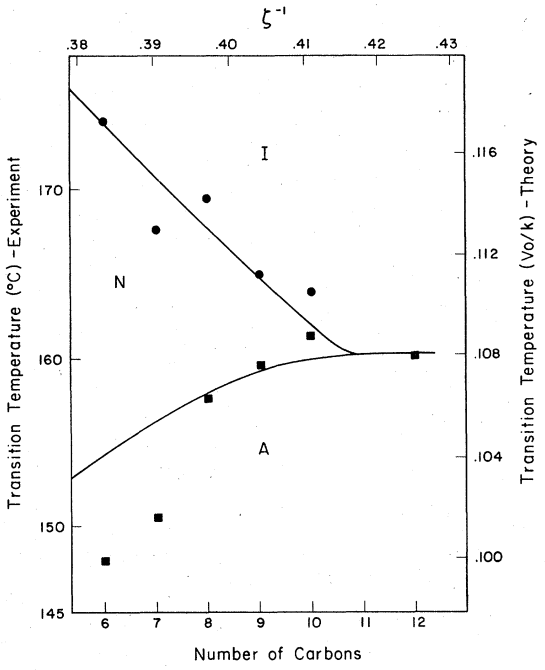

FIG. 7. Comparison of theoretical phase diagram with experiment for 4-n-alkoxybenzylidene-4′-amino-azobenzene. Solid lines are from the theoretical model with $\delta = 0.65$ and $\epsilon = 0.01$. Filled circles and squares denote experimental nematic-isotropic and nematic–smectic-A transition temperatures, respectively, from Ref. 16.

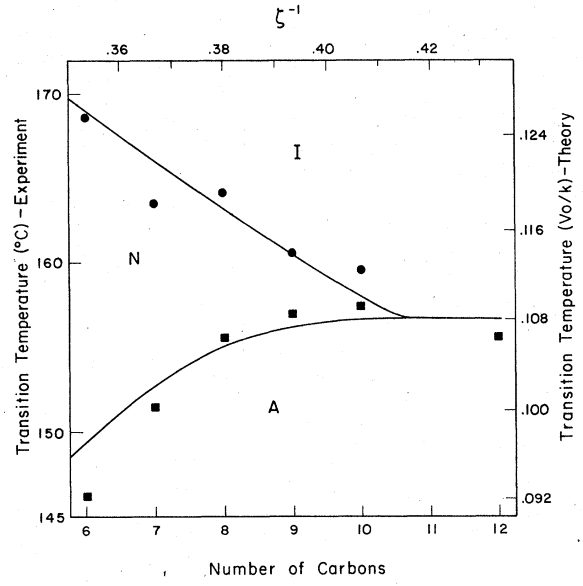

FIG. 6. Comparison of theoretical phase diagram with experiment for 4-p-n-alkoxybenzylidene aminodiphenyls. Solid lines are from the theoretical model with $\delta = 0.65$ and $\epsilon = 0.01$. Filled circles and squares denote experimental nematic-isotropic and nematic–smectic-A transition temperatures, respectively, from Ref. 14.

benzylidene-4′-aminoazobenzene,[16] and 4:4′-di-(p-n-alkoxybenzylidene amino) diphenyls.[14] The results showing theoretical fits superimposed on data are given in Figs. 4–8.

We also calculated order parameters as functions of temperature for several specific combinations of δ and ϵ values and a representative value of ζ^{-1}: 0.40. The graphs are given in Figs. 9–11.

Since most of the qualitative features of the phase transitions have already been satisfactorily described by previous models, the new terms in our interaction essentially bring about only small corrections as expected. Besides getting similar results as in Ref. 3, however, some improvements are observed.

In the present model we made no prior assumption about the relative orientation between the director $\hat{n}$ and the smectic density wave vector $\hat{q}$. The Helmholtz free energy, which is now an implicit function of this relative orientation, indicates that $(\hat{n} \cdot \hat{q}) = 1$ is the only energetically favorable configuration. This differs from previous models in which all relative orientations are energetically degenerate.

We studied the present model for several values of δ. Contrary to the conjecture in Ref. 3, with in-

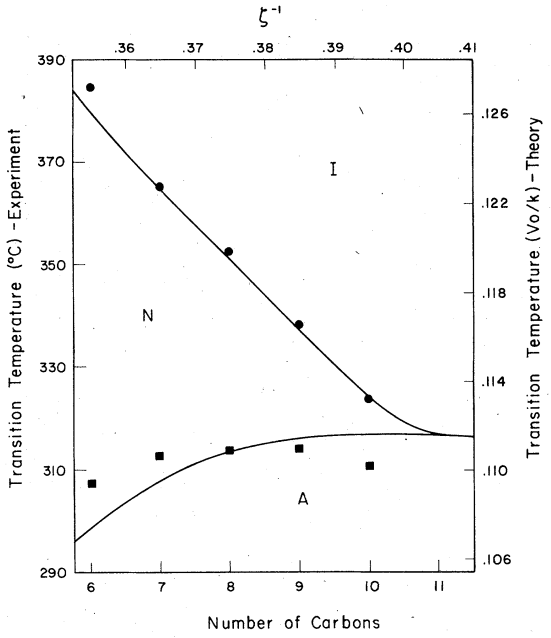

FIG. 8. Comparison of theoretical phase diagram with experiment for 4:4′-di-(*p*-*n*-alkoxybenzylidene amino) diphenyl. Solid lines are from the theoretical model with $\delta = 0.65$ and $\epsilon = 0.05$. Filled circles and squares denote experimental nematic-isotropic and nematic–smectic-*A* transition temperatures, respectively, from Ref. 14.

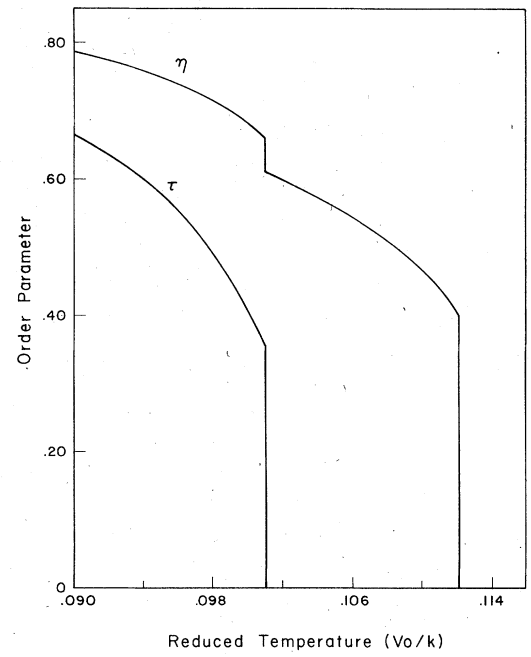

FIG. 9. Orientational order parameter $\eta = \frac{1}{5}\alpha_{0,2}$ and translational order parameter $\tau = \alpha_{1,0}$ vs reduced temperature t for $\delta = 0.45$, $\epsilon = 0.03$, and $\zeta^{-1} = 0.40$.

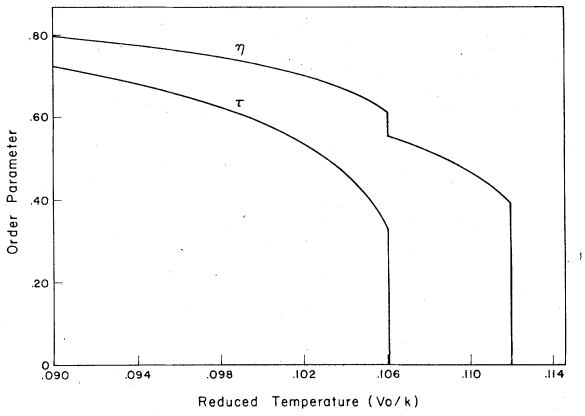

FIG. 10. Orientational order parameter $\eta \equiv \frac{1}{5}\alpha_{0,2}$ and translational order parameter $\tau \equiv \alpha_{1,0}$ vs reduced temperature t for $\delta = 0.65$, $\epsilon = 0$, and $\zeta^{-1} = 0.40$.

creasing δ T_{IA} increases with the length of end chain until it plateaus at some sufficiently long chain length. The value of the parameter δ consistent with experiment varies over the range $0.40 \leq \delta \leq 0.70$ when we consider the model without including steric terms, i.e., when $\epsilon = 0$, which is essentially the model studied in Ref. 3.

The four classes of homologous series whose molecular structures are shown in Fig. 12, all have the same CH=N double bond. The length of the rigid section of the molecules is approximately 10 Å for the first, 15 Å for the second and third, and 20 Å for the last homologous series. This difference in length suggests that each of these homologous series must experience steric forces to a different degree. Indeed, as we make the best possible fits of our results to experimental phase diagrams as shown in Fig. 5–8, we found ϵ increasing with the length of the rigid section of the

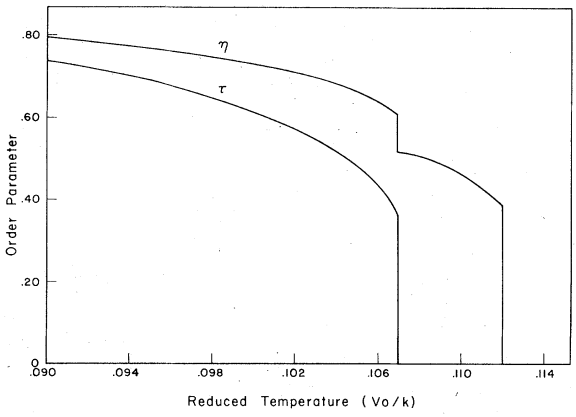

FIG. 11. Orientational order parameter $\eta \equiv \frac{1}{5}\alpha_{0,2}$ and translational order parameter $\tau \equiv \alpha_{1,0}$ for $\delta = 0.65$, $\epsilon = 0.01$, and $\zeta^{-1} = 0.40$.

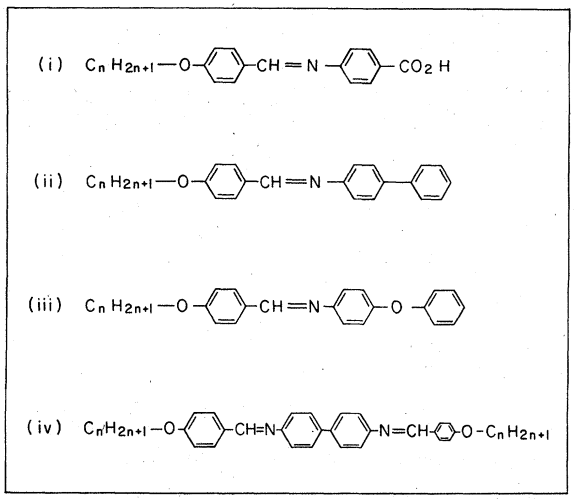

FIG. 12. Molecular structure of the homologous series: (i) p-n-alkoxybenzylidene-p-aminobenzoic acid; (ii) 4-p-n-alkoxybenzylidene aminodiphenyl; (iii) 4-n-alkoxybenzylidene-4′-aminoazobenzene; (iv) 4:4′-Di-(p-n-alkoxybenzylidene amino) diphenyl.

molecule. We have not been able to find more homologous series on which to test our model, but the trend determined with the four available series is certainly encouraging. We conclude that the new terms in the potential, those proportional to $P_2(\hat{\Omega}_1 \cdot \hat{r}_{12})$ do account for steric effects; and furthermore, ϵ does serve as a sensitive measure of the strength of these effects.

It is observed that for a homologous series a single parameter ϵ is sufficient to generate a reasonably good fit to the experimental phase diagram. We might consider this verification of the usual assumption that the excluded volume effect is due mainly to the rigid section of the molecules. The role of the end alkyl chains is merely to cause a larger interplanar spacing ζ^{-1} in the smetic-A phase and thus does not affect the model interaction. In this sense there is now qualitative connection between the parameter ϵ in our model and the molecular structure. We feel that this is an important forward step, since for too long the only way steric effects were considered required the use of hard-rod models, which have had their share of difficulties. The model interaction proposed in this paper appears both simple and effective.

APPENDIX A

Here the various integrals in Eqs. (5.1)–(5.3) are rewritten in forms that can be evaluated by numerical integration. We obtain

$$\int_{\Delta v}\int_{\Omega} \exp\{2\beta_{1,0}\cos(2\pi Z/d)+[\beta_{0,2}+2\beta_{1,2}\cos(2\pi Z/d)]P_2(\hat{n}\cdot\hat{\Omega})\}\,d\vec{r}\,d\hat{\Omega}$$

$$=2\Delta v\int_0^{2\pi}\exp(2\beta_{1,0}\cos\alpha)\left(\int_0^1 \exp[(\beta_{0,2}+2\beta_{1,2}\cos\alpha)(3x^2-1)/2]\,dx\right)d\alpha$$

$$=2\Delta v e^{\beta_{0,2}}\int_0^{2\pi}\exp[2(\beta_{1,0}+\beta_{1,2})\cos\alpha]\,\frac{\mathrm{DAW}([\tfrac{3}{2}(\beta_{0,2}+2\beta_{1,2}\cos\alpha)]^{1/2})\,d\alpha}{[\tfrac{3}{2}(\beta_{0,2}+2\beta_{1,2}\cos\alpha)]^{1/2}}$$

$$\equiv 2\Delta v e^{\beta_{0,2}}\kappa_0(\beta_{0,2},\beta_{1,0},\beta_{1,2}), \tag{A1}$$

where DAW(x) is the Dawson integral,[12] given by

$$\mathrm{DAW}(x)=e^{-x^2}\int_0^x e^{t^2}\,dt. \tag{A2}$$

$$\int_{\Delta v}\int_{\Omega} \exp\{2\beta_{1,0}\cos(2\pi Z/d)+[\beta_{0,2}+2\beta_{1,2}\cos(2\pi Z/d)]P_2(\hat{n}\cdot\hat{\Omega})\}\cos(2\pi Z/d)\,d\vec{r}\,d\hat{\Omega}$$

$$=2\Delta v e^{\beta_{0,2}}\int_0^{2\pi}\exp[2(\beta_{1,0}+\beta_{1,2})\cos\alpha]\cos\alpha\,\frac{\mathrm{DAW}([\tfrac{3}{2}(\beta_{0,2}+2\beta_{1,2}\cos\alpha)]^{1/2})\,d\alpha}{[\tfrac{3}{2}(\beta_{0,2}+2\beta_{1,2}\cos\alpha)]^{1/2}}$$

$$\equiv 2\Delta v e^{\beta_{0,2}}\kappa_{10}(\beta_{0,2},\beta_{1,0},\beta_{1,2}). \tag{A3}$$

$$\int_{\Delta v}\int_{\Omega} \exp\{2\beta_{1,0}\cos(2\pi Z/d)+[\beta_{0,2}+2\beta_{1,2}\cos(2\pi Z/d)]P_2(\hat{n}\cdot\hat{\Omega})\}P_2(\hat{n}\cdot\hat{\Omega})\,d\vec{r}\,d\hat{\Omega}$$

$$=2\Delta v e^{\beta_{0,2}}\int_0^{2\pi}\frac{\exp[2(\beta_{1,0}+\beta_{1,2})\cos\alpha]}{2(\beta_{0,2}+2\beta_{1,2}\cos\alpha)}\left(1-\frac{1+\beta_{0,2}+2\beta_{1,2}\cos\alpha}{[\tfrac{3}{2}(\beta_{0,2}+2\beta_{1,2}\cos\alpha)]^{1/2}}\,\mathrm{DAW}([\tfrac{3}{2}(\beta_{0,2}+2\beta_{1,2}\cos\alpha)]^{1/2})\right)d\alpha$$

$$\equiv 2\Delta v e^{\beta_{0,2}}\kappa_{02}(\beta_{0,2},\beta_{1,0},\beta_{12}). \tag{A4}$$

$$\int_{\Delta v}\int_{\Omega} \exp\{2\beta_{1,0}\cos(2\pi Z/d)+[\beta_{0,2}+2\beta_{1,2}\cos(2\pi Z/d)]P_2(\hat{n}\cdot\hat{\Omega})\}\cos(2\pi Z/d)P_2(\hat{n}\cdot\hat{\Omega})\,d\vec{r}\,d\hat{\Omega}$$

$$=2\Delta v e^{\beta_{0,2}}\int_0^{2\pi}\frac{\exp[2(\beta_{1,0}+2\beta_{1,2})\cos\alpha]\cos\alpha}{2(\beta_{0,2}+2\beta_{1,2}\cos\alpha)}\left(1-\frac{1+\beta_{0,2}+2\beta_{1,2}\cos\alpha}{[\frac{3}{2}(\beta_{0,2}+2\beta_{1,2}\cos\alpha)]^{1/2}}\mathrm{DAW}([\tfrac{3}{2}(\beta_{0,2}+2\beta_{1,2}\cos\alpha)]^{1/2})\right)d\alpha$$

$$\equiv 2\Delta v e^{\beta_{0,2}}\kappa_{12}(\beta_{0,2},\beta_{1,0},\beta_{1,2}). \tag{A5}$$

APPENDIX B

In this appendix F_2 is rewritten in a simpler expression that can easily be evaluated by numerical integration:

$$F_2\equiv\frac{n^2}{32\pi^2}\int f(\vec{r}_1,\hat{\Omega}_1)f(\vec{r}_2,\hat{\Omega}_2)V(1,2)\,d\vec{r}_1\,d\hat{\Omega}_1\,d\vec{r}_2\,d\hat{\Omega}_2. \tag{B1}$$

Write the volume $\mathcal{V}$ of the system as

$$\mathcal{V}=L_xL_yL_z. \tag{B2}$$

In the thermodynamic limit, $\mathcal{V}\to\infty$, $N\to\infty$, with

$$N/\mathcal{V}=\text{constant}=1/\Delta v, \tag{B3}$$

where as mentioned earlier Δv is the volume of a unit cell, and as before we write

$$N\equiv N_xN_yN_z\equiv(L_x/d_x)(L_y/d_y)(L_z/d). \tag{B4}$$

The integrals in F_2 over coordinates x and y are decoupled and can be done easily:

$$\int_{-\infty}^{\infty}\int_{-\infty}^{\infty}\exp[-(x_1-x_2)^2/r_0^2]dx_1\,dx_2=N_x\int_0^{d_x}dx_1\int_{-\infty}^{\infty}\exp(-x^2/r_0^2)dx=N_xd_xr_0\sqrt{\pi},$$

$$\int_{-\infty}^{\infty}\int_{-\infty}^{\infty}\exp[-(y_1-y_2)^2/r_0^2]dy_1\,dy_2=N_y\int_0^{d_y}dy_1\int_{-\infty}^{\infty}\exp(-y^2/r_0^2)dy=N_yd_yr_0\sqrt{\pi}. \tag{B5}$$

The integrals over Z and $\hat{\Omega}$, on the other hand, cannot be done so simply on account of the coupling term β_{12} in $f(Z,\theta)$. We have the following integrals which can again be written in terms of Dawson's integral. First,

$$\int_{-\infty}^{\infty}\exp\left\{2\beta_{10}\left[\cos\left(\frac{2\pi Z}{d}\,1\right)+\cos\left(\frac{2\pi Z}{d}\,2\right)\right]-\frac{(Z_1-Z_2)^2}{r_0^2}\right\}$$

$$\times\int_{\hat{\Omega}_1}\int_{\hat{\Omega}_2}\exp\{[\beta_{02}+\beta_{12}\cos(2\pi Z_1/d)]P_2(\hat{n}\cdot\hat{\Omega}_1)+[\beta_{02}+2\beta_{12}\cos(2\pi Z_2/d)]P_2(\hat{n}\cdot\hat{\Omega}_2)\}d\hat{\Omega}_1d\hat{\Omega}_2\,dZ_1\,dZ_2$$

$$=4N_Zd^2e^{2\beta_{02}}\int_{-\pi}^{\pi}d\xi_1\int_{-\infty}^{\infty}\exp[2(\beta_{10}+\beta_{12})(\cos\xi_1+\cos\xi_2)-(\xi_1-\xi_2)^2/\zeta^2]$$

$$\times\frac{\mathrm{DAW}([\frac{3}{2}(\beta_{02}+2\beta_{12}\cos\xi_1)]^{1/2})\mathrm{DAW}([\frac{3}{2}(\beta_{02}+2\beta_{12}\cos\xi_2)]^{1/2})}{\frac{3}{2}[(\beta_{02}+2\beta_{12}\cos\xi_1)(\beta_{02}+2\beta_{12}\cos\xi_2)]^{1/2}}d\xi_2$$

$$\equiv 4N_Zd^2e^{2\beta_{02}}J_0(\beta_{02},\beta_{10},\beta_{12};\zeta). \tag{B6}$$

Next we consider the term with a factor $P_2(\hat{\Omega}_1\cdot\hat{\Omega}_2)$ in the integrand of Eq. (B1). By the addition theorem of spherical harmonics

$$P_2(\hat{\Omega}_1\cdot\hat{\Omega}_2)=\frac{4\pi}{5}\sum_{m=-2}^{2}Y_2^m(\theta_1,\varphi_1)Y_2^{m*}(\theta_2,\varphi_2), \tag{B7}$$

we find

$$\int_{-\infty}^{\infty}\int \exp\left\{2\beta_{10}\left[\cos\left(\frac{2\pi Z}{d}1\right)+\cos\left(\frac{2\pi Z}{d}2\right)\right]-\frac{(Z_1-Z_2)^2}{r_0^2}\right\}$$

$$\times\int_{\hat{\Omega}_1}\int_{\hat{\Omega}_2}\exp\{[\beta_{02}+2\beta_{12}\cos(2\pi Z_1/d)]P_2(\hat{n}\cdot\hat{\Omega}_1)+[\beta_{02}+2\beta_{12}\cos(2\pi Z_2/d)]P_2(\hat{n}\cdot\hat{\Omega}_2)\}P_2(\hat{\Omega}_1\cdot\hat{\Omega}_2)\,d\hat{\Omega}_1\,d\hat{\Omega}_2\,dZ_1\,dZ_2$$

$$=(2\pi)^2\int_{-\infty}^{\infty}\int\exp\{2\beta_{10}[\cos(2\pi Z_1/d)+\cos(2\pi Z_2/d)]-(Z_1-Z_2)^2/r_0^2\}$$

$$\times\int_{-1}^{1}\exp\{[\beta_{02}+2\beta_{12}\cos(2\pi Z_1/d)]P_2(x)\}P_2(x)\,dx\int_{-1}^{1}\exp\{[\beta_{02}+2\beta_{12}\cos(2\pi Z_2/d)]P_2(y)\}P_2(y)dy\,dZ_1\,dZ_2$$

$$=4N_z d^2 e^{2\beta_{02}}\int_{-\pi}^{\pi}d\xi_1\int_{-\infty}^{\infty}\frac{\exp[(2\beta_{10}+2\beta_{12})(\cos\xi_1+\cos\xi_2)-(\xi_1-\xi_2)^2/\zeta^2]}{4(\beta_{02}+2\beta_{12}\cos\xi_1)(\beta_{02}+2\beta_{12}\cos\xi_2)}$$

$$\times\left(1-\frac{1+\beta_{02}+2\beta_{12}\cos\xi_1}{[\frac{3}{2}(\beta_{02}+2\beta_{12}\cos\xi_1)]^{1/2}}\,\mathrm{DAW}([\tfrac{3}{2}(\beta_{02}+2\beta_{12}\cos\xi_1)]^{1/2})\right)$$

$$\times\left(1-\frac{1+\beta_{02}+2\beta_{12}\cos\xi_2}{[\frac{3}{2}(\beta_{02}+2\beta_{12}\cos\xi_2)]^{1/2}}\,\mathrm{DAW}([\tfrac{3}{2}(\beta_{02}+2\beta_{12}\cos\xi_2)]^{1/2})\right)d\xi_2$$

$$\equiv 4N_z d^2 e^{2\beta_{02}}J_2(\beta_{02},\beta_{10},\beta_{12};\zeta). \tag{B8}$$

Finally, there is the term in F_2 containing the sum $P_2(\hat{\Omega}_1\cdot\hat{r}_{12})+P_2(\hat{\Omega}_2\cdot\hat{r}_{12})$, which is symmetric with respect to interchanging $\hat{\Omega}_1$ and $\hat{\Omega}_2$. We have the addition theorem

$$P_2(\hat{\Omega}\cdot\hat{r}_{12})=\frac{4\pi}{5}\sum_{m=-2}^{2}Y_2^m(\theta_\Omega,\varphi_\Omega)Y_2^m{}^*(\theta_{12},\varphi_{12}), \tag{B9}$$

where $(\theta_\Omega,\varphi_\Omega)$ and $(\theta_{12},\Omega_{12})$ are the angles which $\hat{\Omega}$ and $\hat{r}_{12}$ make with $\hat{n}$, respectively. Moreover, since $Z_{12}=Z_1-Z_2=r_{12}\cos\theta_{12}$ we have

$$\cos(2\pi Z_2/d)=\cos[2\pi Z_1/d-(2\pi r_{12}/d)\cos\theta_{12}]. \tag{B10}$$

Using Eqs. (B9) and (B10) we obtain for the term containing $P_2(\hat{\Omega}_1\cdot\hat{r}_{12})$:

$$\int_{-\infty}^{\infty}\int\exp\{2\beta_{10}[\cos(2\pi Z_1/d)+\cos(2\pi Z_2/d)]-r_{12}^2/r_0^2\}$$

$$\times\int_{\hat{\Omega}_1}\int_{\hat{\Omega}_2}\exp\{[\beta_{02}+2\beta_{12}\cos(2\pi Z_1/d)]P_2(\hat{\Omega}_1\cdot\hat{n})+[\beta_{02}+2\beta_{12}\cos(2\pi Z_2/d)]P_2(\hat{n}\cdot\hat{\Omega}_2)\}P_2(\hat{\Omega}_1\cdot\hat{r}_{12})d\hat{\Omega}_1\,d\hat{\Omega}_2\,d\vec{r}_1\,d\vec{r}_2$$

$$=4\frac{d^3\mathcal{V}}{(2\pi)}e^{2\beta_{02}}\int_{-\pi}^{\pi}d\xi_1\frac{\exp[(2\beta_{10}+2\beta_{12})\cos\xi_1)}{2(\beta_{02}+2\beta_{12}\cos\xi_1)}\times\left(1-\frac{1+\beta_{02}+2\beta_{12}\cos\xi_1}{[\frac{3}{2}(\beta_{02}+2\beta_{12}\cos\xi_1)]^{1/2}}\,\mathrm{DAW}([\tfrac{3}{2}(\beta_{02}+2\beta_{12}\cos\xi_1]^{1/2})\right)$$

$$\times\int_0^{\infty}\xi^2e^{-\xi^2/\zeta^2}\,d\xi\int_{-1}^{1}\exp[(2\beta_{10}+2\beta_{12})\cos(\xi_1+\xi x)]P_2(x)\,\frac{\mathrm{DAW}(\{\frac{3}{2}[\beta_{02}+2\beta_{12}\cos(\xi_1+\xi x)]\}^{1/2})}{\{\frac{3}{2}[\beta_{02}+2\beta_{12}\cos(\xi_1+\xi x)]\}^{1/2}}dx$$

$$\equiv 4\frac{d^3\mathcal{V}}{(2\pi)}e^{2\beta_{02}}J_3(\beta_{02},\beta_{10},\beta_{12};\zeta). \tag{B11}$$

By symmetry the integral containing $P_2(\hat{\Omega}_2\cdot\hat{r}_{12})$ gives the same result.

Collecting terms from Eqs. (B5), (B6), (B8), and (B11), we obtain

$$F_2=kTN\frac{\zeta_x\zeta_y}{4\pi t[\kappa_0(\beta_{02},\beta_{10},\beta_{12})]^2}[-\tfrac{1}{2}\delta J_0(\beta_{02},\beta_{10},\beta_{12};\zeta)-\tfrac{1}{2}J_2(\beta_{02},\beta_{10},\beta_{12};\zeta)+(2\epsilon/\zeta^2)J_3(\beta_{02},\beta_{10},\beta_{12};\zeta)]. \tag{B12}$$

*Work supported in part by the NSF through Grant No. DMR76-18375.

[1]K. K. Kobayashi, J. Phys. Soc. Jpn. 29, 101 (1970); Mol. Cryst. Liq. Cryst. 13, 137 (1971).
[2]W. L. McMillan, Phys. Rev. A 4, 1238 (1971); 6, 936 (1972).
[3]F. T. Lee, H. T. Tan, Y. M. Shih, and C.-W. Woo, Phys. Rev. Lett. 31, 1117 (1973).
[4]W. Maier and A. Saupe, Z. Naturforsch. A 13, 564 (1958); 14, 882 (1959), 15, 287 (1960).
[5]R. G. Priest (unpublished); C. T. Chen-Tsai (private communication).
[6]J. A. Pople, Proc. R. Soc. A 221, 498 (1954).
[7]L. Shen, H. K. Sim, Y. M. Shih, and C.-W. Woo, Mol. Cryst. Liq. Cryst. (to be published).
[8]C. W. Oseen, Trans. Faraday. Soc. 29, 883 (1933).
[9]Y. R. Lin-Liu, Y. M. Shih, and C.-W. Woo, Phys. Rev. A 14, 445 (1976).
[10]E. Merzbacher, *Quantum Mechanics* (Wiley, New York, 1970), p. 198.
[11]M. A. Abramowitz and T. A. Segun, *Handbook of Mathematical Functions* (Dover, New York, 1968), p. 505.
[12]Reference 11, p. 319.
[13]H. Arnold, Z. Phys. Chem. (Leipz.) 239, 283 (1968).
[14]J. S. Dave and P. R. Patel, Mol. Cryst. Liq. Cryst. 2, 115 (1966).
[15]G. W. Gray, J. B. Hartley, A. Ibbotson, and Brynmor Jones, J. Chem. Soc. (Lond.) 4359 (1955).
[16]D. L. Fishel and P. R. Patel, Mol. Cryst. Liq. Cryst. 17, 139 (1972).